

Collective modes of a helical liquid

S. Raghu, Suk Bum Chung, Xiao-Liang Qi and Shou-Cheng Zhang

Department of Physics, McCullough Building, Stanford University, Stanford, CA 94305-4045

(Dated: October 31, 2018)

We study low energy collective modes and transport properties of the “helical metal” on the surface of a topological insulator. At low energies, electrical transport and spin dynamics at the surface are exactly related by an operator identity equating the electric current to the in-plane components of the spin degrees of freedom. From this relation it follows that an undamped spin wave always accompanies the sound mode in the helical metal – thus it is possible to ‘hear’ the sound of spins. In the presence of long range Coulomb interactions, the surface plasmon mode is also coupled to the spin wave, giving rise to a hybridized “spin-plasmon” mode. We make quantitative predictions for the spin-plasmon in Bi_2Se_3 , and discuss its detection in a spin-grating experiment.

PACS numbers: 71.10.Ay, 71.45.-d, 71.45.Gm, 72.15.Nj, 73.20.Mf, 73.20.-r, 73.25.+i, 73.43.Lp

Introduction - Recently, topological insulators have been theoretically predicted and experimentally observed in both quasi-two dimensional (2D) and three dimensional (3D) systems[1, 2, 3, 4, 5, 6, 7]. The concept of a topological insulator can be defined within the non-interacting topological band theory[8, 9] or more generally within the topological field theory[10], which is also valid for interacting systems. The simplest topological insulators such as Bi_2Se_3 and Bi_2Te_3 have a full bulk insulating gap and a surface state consisting of a single Dirac cone[5, 6, 7]. As is the case for the helical edge states of a 2D topological insulator[11, 12], the spin and the momentum are intimately locked in the “helical metal” surface state of the 3D topological insulator. This locking effect has been theoretically predicted[6] for Bi_2Se_3 and Bi_2Te_3 , and experimentally observed[19] in Bi_2Se_3 .

In this paper, we study the universal surface state properties of the simplest 3D topological insulators, and consider a system governed by a single isotropic Dirac cone at energy scales much lower than the bulk insulating gap. We study the consequences of the helical nature of the metallic states: the coupling between spin and charge excitations, and collective modes of the helical liquid. Our theory here is directly applicable to the case of the $\text{Bi}_2\text{Se}_3/\text{Bi}_2\text{Te}_3$ family, which has a single isotropic Dirac cone that remains isotropic for low dopant concentrations.

Spin dynamics and electrical transport - Starting from a low energy effective Hamiltonian for the bulk of a 3D topological insulator in the Bi_2Se_3 family, the low energy surface Hamiltonian was derived by Zhang *et al.* [6] by diagonalizing the bulk effective Hamiltonian with open boundary conditions, and by integrating out the high energy bulk degrees of freedom. In Ref. [6], it was shown that for a surface in the xy-plane, the helical states at low energies are governed by

$$H = \int d^2\mathbf{x} \psi^\dagger(\mathbf{x}) [\hbar v_f (\hat{\mathbf{z}} \times (-i\nabla)) \cdot \boldsymbol{\sigma} - \mu] \psi(\mathbf{x}), \quad (1)$$

where \mathbf{k} is the Bloch vector in the 2D surface Brillouin

zone and $\boldsymbol{\sigma}$ the Pauli matrices describing electron spin. Here, μ is the value of the chemical potential relative to the surface Dirac point. This Hamiltonian adequately captures the dynamics of the surface for energies much smaller than the bulk gap Δ , and for length scales much larger than $\hbar v_f/\Delta$, the penetration depth of the gapless surface states into the bulk. In this regime, there are several universal features that characterize the surface states. First there is the operator identity relating the charge current to the in-plane component of the spin on the surface:

$$\mathbf{j}(\mathbf{x}) = \psi^\dagger(\mathbf{x}) v_f (\boldsymbol{\sigma} \times \hat{\mathbf{z}}) \psi(\mathbf{x}) \equiv v_f \mathbf{S}(\mathbf{x}) \times \hat{\mathbf{z}} \quad (2)$$

Such a simple relation between charge current density and spin density is the key observation of this work, which is a unique property of the helical liquid, and leads to many intrinsic correspondences between spin and charge dynamics in the system. It should be noticed that the operator identity Eq. (2) remains valid even when interaction terms are added to the Hamiltonian. The only deviation from this identity comes from the change of Fermi surface shape due to rotational symmetry breaking, which has been observed in Bi_2Te_3 when the chemical potential is close to the bottom of the bulk conduction band [7]. In this regime, the Fermi velocity obtains an $O(k/k_f)^2$ distortion[13, 14], and the operator identity above no longer rigorously holds. However, there is still a one-to-one correspondence between the velocity and spin of the surface electrons, so that many conclusions we will discuss in the following will still hold qualitatively in this regime.

In what follows, we will assume a perfectly circular fermi surface in the continuum limit. From the above identity (2), we derive the important dynamical identity between correlation functions

$$v_f^2 \epsilon_{ik} \epsilon_{jl} \langle T_\tau s_i(\tau) s_j(0) \rangle = \langle T_\tau j_k(\tau) j_l(0) \rangle \quad (3)$$

which relates the electric transport to the dynamical spin structure factor in the linear response regime. The electric response of the helical metal can thus be calculated

from the generalized spin and density susceptibility

$$\chi_{\mu\nu}(\mathbf{q}, i\Omega_m) = \frac{-1}{\beta} \sum_{\mathbf{k}, i\omega_n} \text{Tr}[\sigma_\mu \mathcal{G}(\mathbf{k} + \mathbf{q}, i\omega_n + i\Omega_m) \sigma_\nu \mathcal{G}(\mathbf{k}, i\omega_n)], \quad (4)$$

where $\sigma_\mu = (1, \boldsymbol{\sigma})$, and we have introduced the Matsubara Green function \mathcal{G} . In particular, the optical conductivity $\sigma_{xx}(\omega)$ is simply related to dynamical spin susceptibility: $\sigma_{xx}(\omega) = \frac{i}{\omega} v_f^2 \chi_{yy}(\omega)$, while the Hall conductivity is related to the off-diagonal dynamical spin susceptibility $\sigma_{xy}(\omega) = -\frac{i}{\omega} v_f^2 \chi_{yx}(\omega)$. In principle, this relation can be verified by comparing the optical conductivity with the experimental results of spin-polarized neutron or polarized light scattering.

Due to the rotational invariance of the Fermi surface about the \hat{z} axis, the longitudinal ($s^L = \hat{\mathbf{q}} \cdot \mathbf{s}$) and transverse ($s^T = \hat{\mathbf{z}} \cdot (\hat{\mathbf{q}} \times \mathbf{s})$) components of the spin excitations are decoupled. In particular, it can be shown that susceptibilities involving correlations between longitudinal and transverse spin degrees of freedom vanish identically. An explicit evaluation of Eq.(4) shows that the 4×4 susceptibility tensor decomposes into two 2×2 matrices, one with the density and transverse spin, and the other with the perpendicular (s_z) and the longitudinal spin. The density-transverse spin block of the susceptibility tensor can be determined from the Ward identity that has its origin in the continuity equation for the density: $\partial_t n_{\mathbf{q}} = -iqj_{\mathbf{q}}^L$, where $j_{\mathbf{q}}^L = \hat{\mathbf{q}} \cdot \mathbf{j}_{\mathbf{q}}$ is the longitudinal current. The Ward identity, combined with the operator identity in Eq.(2) gives us

$$\partial_t n_{\mathbf{q}} = -iqs_{\mathbf{q}}^T. \quad (5)$$

We note that the longitudinal current is simply the transverse spin degree of freedom.

The structure of the density and spin response bears a remarkable resemblance to source-free Maxwell electrodynamics in $2 + 1$ dimensions, as first pointed out in Ref. [15]. The analogy is made precise when we identify the density with the “magnetic field” perpendicular to the surface, and the transverse spin components with the “electric field” in the plane of the surface. Eq. (5) can be written as $\partial_t n = -\nabla \times \mathbf{s}^T$ in the real space. The equation of continuity that connects the density to the transverse spin is thus precisely the Faraday law for this system. Moreover, Gauss’ law for the electric field $\nabla \cdot \mathbf{s}^T = 0$ is satisfied by construction, since the spins are transverse to the in-plane momentum. A similar identification has been made for a system with Rashba spin-orbit coupling [15]; however, the analogy to electrodynamics is less precise in Rashba systems than in the case of the helical metal due to the presence of the quadratic dispersion in the Rashba Hamiltonian.

Applying the Ward identity to the response functions, we find that the density and transverse spin subset of the

susceptibility tensor in the basis (n, s^T) has the form

$$\chi = \begin{pmatrix} 1 & x \\ -x & -x^2 \end{pmatrix} \chi_{nn}, \quad x = \frac{\omega}{v_f q} \quad (6)$$

We note that in order to obtain this form, we need to regularize the susceptibility tensor, taking the $\mu = 0$ ground state as the vacuum [16, 17].

The bare susceptibilities can be evaluated explicitly for arbitrary ω and q using the non-interacting Green function

$$\begin{aligned} \mathcal{G}^{(0)}(\mathbf{k}, i\omega_n) &= [i\omega_n - \mathcal{H}(\mathbf{k})]^{-1} = \sum_{s=\pm 1} \mathcal{P}_s G_s^{(0)}(i\omega_n, \mathbf{k}), \\ \mathcal{P}_s &= \frac{1}{2} [1 + s(\hat{\mathbf{z}} \times \hat{\mathbf{k}}) \cdot \boldsymbol{\sigma}], \\ G_s^{(0)} &= [i\omega_n - sv_f k + \mu]^{-1} \end{aligned} \quad (7)$$

As shown in Fig. 1, we find that particle-hole excitations are found everywhere except for $v_f q < \omega < 2\mu - v_f q$. In this region, the imaginary components of all the susceptibilities vanish and collective excitations are undamped.

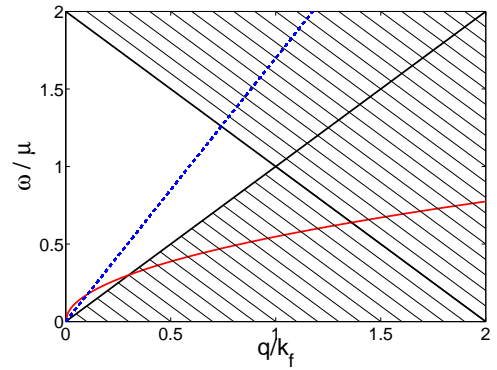


FIG. 1: Dispersion of the collective modes in the long wavelength regime. The plasmon (solid red line) is shown for $\alpha = 0.6$ and the zero-sound (dashed blue line) mode is shown for $U = 0.3U_c$. The shaded region denotes the particle-hole continuum where the imaginary parts of the density and spin susceptibilities are non-zero. The collective modes are long-lived in the unshaded region $v_f q < \omega < 2\mu - v_f q$.

Collective modes - In the long-wavelength, low frequency limit, $q \ll k_f, \omega \ll \mu$, the non-interacting density susceptibility to leading order is

$$\chi_{nn} = \frac{\mu}{2\pi\hbar^2 v_f^2} \left[\frac{x}{\sqrt{x^2 - 1}} - 1 \right], \quad x = \frac{\omega + i\delta}{v_f q} \quad (8)$$

with corrections $O(q/k_f)^2$. Thus, for $\omega > v_f q$, the imaginary part of the density and spin susceptibilities vanish and undamped collective modes exist. To determine the collective mode spectrum in this regime, we treat the susceptibility tensor within the random phase approximation (RPA).

In the case of the long-ranged Coulomb interaction, $U(q)$, the RPA correction to the susceptibilities in Eq.(6) is given by

$$\hat{\chi}^{RPA}(\mathbf{q}, \omega + i\delta) = \hat{\chi} \left[\hat{1} - \frac{U(q)}{2} (\hat{1} + \hat{\tau}^z) \hat{\chi} \right]^{-1} \quad (9)$$

where $\hat{\chi}$ is the density and transverse spin susceptibility in Eq.(6) and τ^z is a Pauli matrix in the same basis. Although the susceptibility is a 2×2 matrix, the result of the RPA correction turns out to be the same as an ordinary 2D Fermi liquid:

$$\hat{\chi}_{RPA} = \begin{pmatrix} 1 & x \\ -x & -x^2 \end{pmatrix} \frac{\chi_{nn}}{1 - U\chi_{nn}}, \quad x = \frac{\omega}{v_f q} \quad (10)$$

Collective mode excitation spectra are obtained via the poles of the matrix of RPA susceptibilities. For the Coulomb interaction $U(q) = 2\pi\hbar\alpha v_f/q$, where $\alpha = e^2/\epsilon_d\hbar v_f$ (ϵ_d being the dielectric constant of the topological insulator) is the fine structure constant for the helical metal. Therefore the plasmon dispersion satisfies

$$\frac{\hbar v_f q}{\alpha\mu} = \frac{x}{\sqrt{x^2 - 1}} - 1 \quad (11)$$

which for small q establishes that plasmon modes are gapless and propagate with a dispersion

$$\omega = \frac{\mu}{\hbar} \sqrt{\frac{\alpha}{2} \frac{q}{k_f}}, \quad (12)$$

similar to an ordinary Fermi liquid in 2D. Note that in order for the plasmon to propagate, the solution to Eq.(11) needs to stay in the unshaded region of Fig. 1, which means that for frequency above $\omega_c = (\alpha/2)(\mu/\hbar)$, the plasmon will merge into the particle-hole continuum. We expect $\hbar\omega_c \sim 2.2\text{meV}$ for the Bi_2Se_3 family; this comes from $\epsilon_d \approx 100$ [18] and $v_f \approx 5.0 \times 10^5\text{m/s}$ with μ typically around 100meV [5, 19].

In sharp contrast to the conventional Fermi liquid, the surface plasmon of the helical liquid always carries spin, and could be appropriately called the *spin-plasmon*. This is a consequence of the equation of continuity for the density and the operator identity, Eq. 2: $\partial_t n_{\mathbf{q}} = -iqs_{\mathbf{q}}^T$. Thus, a fluctuation in the density will be accompanied by a transverse spin fluctuation due to the ‘‘Faraday law’’ that couples them. In Fig. 2, the nature of the spin-plasmon is shown pictorially at a fixed ω and q . A density oscillation induces a transverse spin wave in perfect analogy with Maxwell electrodynamics in $2 + 1$ dimensions. At the peaks and troughs of the density wave, the transverse spin components are zero, whereas regions where the density variations vanish are accompanied by a maximum spin polarization. The locking of the spin and charge degrees of freedom in the spin-plasmon collective mode is unique to the helical liquid and marks a striking difference relative to the ordinary Fermi liquid.

For short-ranged Hubbard-like interactions, the RPA susceptibilities are

$$\hat{\chi}^{RPA}(\mathbf{q}, \omega + i\delta) = \hat{\chi} [\hat{1} - U\hat{\tau}^z\hat{\chi}]^{-1} \quad (13)$$

The reason for this difference in the RPA susceptibilities is that short ranged Hubbard-like interactions can be decomposed in both the density and spin channels, both of which contribute to RPA diagrams, whereas the Coulomb interaction can only be decomposed in the charge channel in the RPA approximation. In both cases, the RPA susceptibilities satisfy the Ward identity.

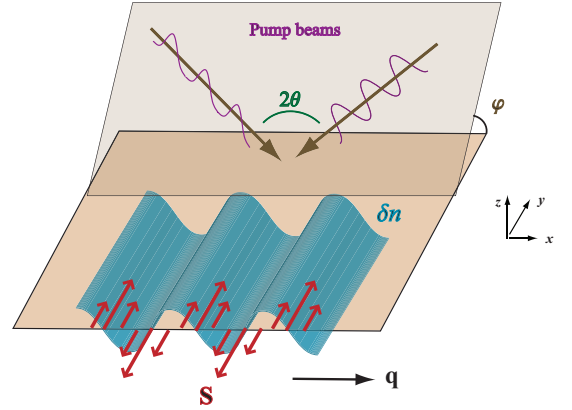


FIG. 2: The spin-plasmon collective mode: a density fluctuation (green surface) induces a transverse spin fluctuation (red arrows) or *vice-versa*. To detect the spin-plasmon, a spin-density wave is generated by a spin grating. Two orthogonally polarized non-collinear incident beams (relative angle of 2θ) induce a spin polarization wave. The transverse component of the photon helicity is $P \cos \theta \cos \varphi$ where P is the total photon helicity amplitude and φ is the beam plane makes with the surface. The induced plasmon charge oscillation can be detected by conventional means.

The zero sound spectra for short range interaction can be determined by the pole of Eq. (13), which is given by

$$\frac{2\pi\hbar^2 v_f^2}{U\mu} = (x^2 + 1) \left(\frac{x}{\sqrt{x^2 - 1}} - 1 \right) \quad (14)$$

In this case, there is an essential difference from the ordinary fermi liquid. The right hand side of Eq. (14) takes its value in the range $[\frac{1}{2}, +\infty)$, so that the equation has a solution only if $4\pi\hbar^2 v_f^2/U\mu > 1$, or $U < U_c = 4\pi\hbar^2 v_f^2/\mu$. The sound wave dispersion for the two limiting cases $U \ll U_c$ and $U \lesssim U_c$ are

$$\omega = \begin{cases} v_f q \left(1 + \frac{8U^2}{U_c^2} \right), & U/U_c \rightarrow 0 \\ v_f q \sqrt{\frac{7}{4} \frac{U}{U_c - U}}, & U/U_c \rightarrow 1 \end{cases} \quad (15)$$

Physically, the disappearance of the sound mode for strong interaction $U > U_c$ can be understood as a consequence of the attractive interaction in the spin channel:

note that the interaction vertex in Eq. (13) for the density correlation χ_{nn} has the opposite sign of the vertex for the transverse spin correlation χ_{TT} . In an ordinary Fermi liquid with repulsive short range interaction, the same argument leads to the damping of the spin wave, but does not affect the zero sound since the spin and charge response are decoupled (or only weakly coupled in systems with weak to moderate spin-orbit coupling). By contrast, in the helical spin liquid, the spin and charge responses are intrinsically coupled due to the operator identity Eq. (2), so that the sound wave can be damped even for a repulsive interaction.

Spin grating measurements - Our basic method of detecting the spin-plasmon mode is to excite the spin degree of freedom and to detect the propagating density wave coupled to the spin polarization wave. In other words, we generate transverse spin polarization and detect the induced density wave, which we can measure through spatial modulation of reflectivity.

For generating the transverse spin wave, we propose a method similar to the transient spin grating (TSG) used in Refs. 20 and 21. For our version of TSG, shown in Fig. 2, we need to have two non-collinear femtosecond laser beam pulses incident on the topological insulator surface, with $\hat{\mathbf{z}}$ set as the surface normal; the wave vector directions of these two beams are $(\pm \sin \theta, -\cos \theta \cos \varphi, -\cos \theta \sin \varphi)$. By linearly polarizing the two beams in orthogonal directions, we can generate by interference alternating photon helicity in the direction $(\sin \theta, -\cos \theta \cos \varphi, -\cos \theta \sin \varphi)$ with the grating vector \mathbf{q} along $\hat{\mathbf{x}}$; the q can be varied by changing the relative phase between the two interfering beams. For the persistent spin helix experiment, Ti:sapphire lasers (wavelength 650~1100nm) were used to obtain $q = 0.34 - 2.5 \times 10^4 \text{cm}^{-1}$ [21]; this q value would suit our purpose (a typical k_f with μ lying in the bulk gap can be taken as $60 \times 10^4 \text{cm}^{-1}$ for Bi_2Se_3 or Bi_2Te_3 [5, 7]). So long as we keep the two beams' polarization orthogonal and intensity equal, this photon helicity wave does not directly generate any density wave. However, the spin polarization wave it generates will have a nonzero $s^T \propto \cos \theta \cos \varphi$ for $\varphi \neq \pi/2$. After the laser pulses are applied, the transverse spin components s^T propagate through the spin-plasmon collective mode. On the other hand, other spin components are Landau damped. Note that intensity I of the induced density-spin wave has φ dependence, which vanishes for $\varphi = \pi/2$ since in that case $s^T = 0$. Observation of such dependence would be a strong evidence confirming our helical liquid theory.

In conclusion we presented a general theory of the collective modes of the helical liquid. We derived a general relation between the charge current and the spin which is valid for arbitrarily interacting systems. We show that the spin-plasmon mode propagates on the surface of a topological insulator, and propose a experimental setting to detect this mode. The spin-plasmon mode uni-

fies spintronics and plasmonics, two frontier branches of current research, and can be used for spin transport in spintronics devices.

We are grateful to Mark Brongersma, Kai Chang, Run-Dong Li and Joseph Orenstein for insightful discussions. This work is supported by the Department of Energy, Office of Basic Energy Sciences, Division of Materials Sciences and Engineering, under contract DE-AC02-76SF00515, and by the Stanford Institute for Theoretical Physics (SITP) postdoctoral fellowship (SR and SBC). Part of this work was carried out at the Kavli Institute for Theoretical Physics, UC Santa Barbara, with support from KITP's NSF Grant No. PHY05-51164.

-
- [1] B. A. Bernevig, T. L. Hughes, and S.-C. Zhang, *Science* **314**, 1757 (2006).
 - [2] M. König, S. Wiedmann, C. Brune, A. Roth, H. Buhmann, L. Molenkamp, X.-L. Qi, and S.-C. Zhang, *Science* **318**, 766 (2007).
 - [3] L. Fu and C. L. Kane, *Phys. Rev. B* **76**, 045302 (2007).
 - [4] D. Hsieh, D. Qian, L. Wray, Y. Xia, Y. S. Hor, R. J. Cava, and M. Z. Hasan, *Nature* **452**, 970 (2008).
 - [5] Y. Xia, D. Qian, D. Hsieh, L. Wray, A. Pal, H. Lin, A. Bansil, D. Grauer, Y. S. Hor, R. J. Cava, et al., *Nature Physics* **5**, 398 (2009).
 - [6] H. Zhang, C. Liu, X.-L. Qi, X. Dai, Z. Fang, and S.-C. Zhang, *Nature Physics* **5**, 438 (2009).
 - [7] Y. L. Chen, J. G. Analytis, J. H. Chu, Z. K. Liu, S. K. Mo, X. L. Qi, H. J. Zhang, D. H. Lu, X. Dai, Z. Fang, et al., *Science* **325**, 178 (2009).
 - [8] J. E. Moore and L. Balents, *Phys. Rev. B* **75**, 121306 (2007).
 - [9] L. Fu, C. L. Kane, and E. J. Mele, *Phys. Rev. Lett.* **98**, 106803 (2007).
 - [10] X.-L. Qi, T. Hughes, and S.-C. Zhang, *Phys. Rev. B* **75**, 121306 (2007).
 - [11] C. Xu and J. Moore, *Phys. Rev. B* **73**, 045322 (2006).
 - [12] C. Wu, B.A. Bernevig, and S.C. Zhang, *Phys. Rev. Lett.* **96**, 106401 (2006).
 - [13] L. Fu, arXiv:0908.1418 (2009).
 - [14] Z. Alpichshev, J. Analytis, J.-H. Chu, I. Fisher, Y. L. Chen, Z. X. Shen, A. Fang, and A. Kapitulnik, arXiv:0908.0371 (2009).
 - [15] B. A. Bernevig, X. Yu, and S.-C. Zhang, *Phys. Rev. Lett.* **95**, 076602 (2005).
 - [16] M. Polini, A. H. MacDonald, and G. Vignale, arXiv:0901.4528 (2009).
 - [17] A. Principi, M. Polini, and G. Vignale, *Phys. Rev. B* **80**, 075418 (2009).
 - [18] W. Richter and C. R. Becker, *Physica Status Solidi (b)* **84**, 619 (1977).
 - [19] D. Hsieh, Y. Xia, D. Qian, L. Wray, J. H. Dil, F. Meier, J. Osterwalder, L. Patthey, J. G. Checkelsky, N. P. Ong, et al., *Nature* **460**, 1101 (2009).
 - [20] C. P. Weber, J. Orenstein, B. A. Bernevig, S.-C. Zhang, J. Stephens, and D. D. Awschalom, *Phys. Rev. Lett.* **98**, 076604 (2007).
 - [21] J. D. Koralek, C. P. Weber, B. A. Bernevig, S.-C. Zhang, S. Mack, and D. D. Awschalom, *Nature* **458**, 610 (2009).